Phase synchronization of electroencephalographic signals in the different frequency bands

M. C. Faustino[1], R. P. Serquiña[2], P. E. Rapp[3], A. M. Albano[4]*

[1] Department of Mathematics, Xavier University, Cagayan de Oro City, Philippines.
[2] Department of Mathematics and Statistics, Mindanao State University – Iligan Institute of Technology, Iligan City, Philippines.
[3] Department of Military and Emergency Medicine, Uniformed Services University, Bethesda, MD 20814 USA.
[4] Department of Physics, Bryn Mawr College, Bryn Mawr, PA 19010 USA.

We use Kuramoto's parameter ρ to evaluate the phase synchronization of multichannel EEG records at different frequency bands for thirteen human subjects under two behavioral conditions: eyes open resting and eyes closed resting. We report three findings: (1) with eyes open, the dependence of ρ on frequency can be described by a 7th order polynomial, and with the eyes closed, by a 6th order polynomial; (2) for all frequency bands, pair-wise synchronization between channels is inversely proportional to inter-electrode distance; and (3) although there are visible differences in average synchronization between behavioral conditions, inter-subject variations are so great such that the differences are not statistically significant.

*Corresponding author
Email Address: aalbano@brynmawr.edu
Submitted: March 28, 2012
Revised: June 19, 2012
Accepted: June 20, 2012
Published: September 18, 2012
Editor-in-charge: Eduardo A. Padlan

KEYWORDS

Neuroscience, EEG, phase synchronization, functional connectivity, Kuramoto order parameter

INTRODUCTION

The connectivity of the brain has long been an important focus of studies of the human central nervous system. Earlier work had concentrated on anatomical connectivity which traced how different regions are connected to each other by neuronal projections. These projections indicate which regions are capable of directly communicating with each other without, however, providing information about actual patterns of communication in the functioning brain or about how these patterns change with changes in brain activity. Studies of functional connectivity seek to uncover and to understand these patterns.

Early attempts used the cross-correlation coefficient to measure linear correlations of EEG signals from different scalp sites (Imahori and Suhara 1949, cited by Gevins and Remond 1987; Brazier and Casby 1952). Fraser and Swinney (1986) and Mars and Lopes da Silva (1987) later showed that mutual information is capable of evaluating nonlinear correlations not detected by linear measures. This measure has since been used in similar contexts by others (Xu et al. 1997; Albano et al. 2000). Going beyond correlations, causality measures or measures of information transfer such as Granger causality (1969) and transfer entropy (Schreiber 2000; Albano et al. 2008; Madulara

et al. 2012) show how one data stream influences the evolution of another.

The frequency dependence of linear correlations is often studied by means of spectral coherence, the Fourier transform of the covariance function (von Stein and Sarnthein 2000). Another approach, which we use here, is to subject the raw EEG signal to bandpass filters and then study the correlations of the filtered data.

The measures discussed above typically evaluate relationships of the amplitudes of pairs of data streams. Instead of relying on amplitudes, one may instead associate phases with real-valued signals using, say, the Hilbert Transform (Hahn 1996; King 2009). The synchronization of the phases of multi-channel data may then be calculated. Kuramoto's parameter, ρ (see below), is a particularly useful measure of the all-to-all phase synchronization of these data (Kuramoto 1975, 1984; Sakaguchi and Kuramoto 1986; Strogatz 2000; Acebrón et al. 2005).

Using Kuramoto's ρ we investigate the dependence on frequency and on inter-electrode distance of the phase synchronization of 10-channel, free-running EEG for two behavioral conditions: eyes closed resting and eyes open resting. This gives us the opportunity to compare spontaneous synchronization of the different brain regions when the visual system is activated to that when it is not. This is to be contrasted with the approach of some previous works which studied the amplitude correlations of EEG when subjects were performing tasks that are thought to involve a variety of neuronal assemblies (e.g., von Stein and Sarnthein 2000).

We find that (1) phase synchronization is a rather complicated function of frequency, best represented, for the eyes open and eyes closed cases, by 7th and 6th order polynomials, respectively; (2) on average, for all frequency bands, ρ is inversely proportional to inter-electrode distance; and (3) although values of ρ averaged over all subjects show systematic differences for the two behavioral conditions, inter-subject variations in each condition are so great that there are no statistically significant differences in synchronization among the different frequency bands for each condition. Neither are there significant differences in synchronization between conditions.

FREQUENCY BANDS, FILTERING, AND PHASE SYNCHRONIZATION

Electroencephalographic frequency bands

The frequencies of EEG signals usually range from less than 1 to about 60 Hz, and have amplitudes that range from 29 to 100μV. In the state of consciousness, EEG waves have certain characteristic patterns at the highest state of alertness, when sensory input is at the greatest; the waves are of high frequency and low amplitude. At the opposite end of the alertness scale, a synchronized EEG has the characteristics of low frequency and high amplitude.

EEG wave patterns are classified according to their frequency, *f*, each frequency band having its own physiological

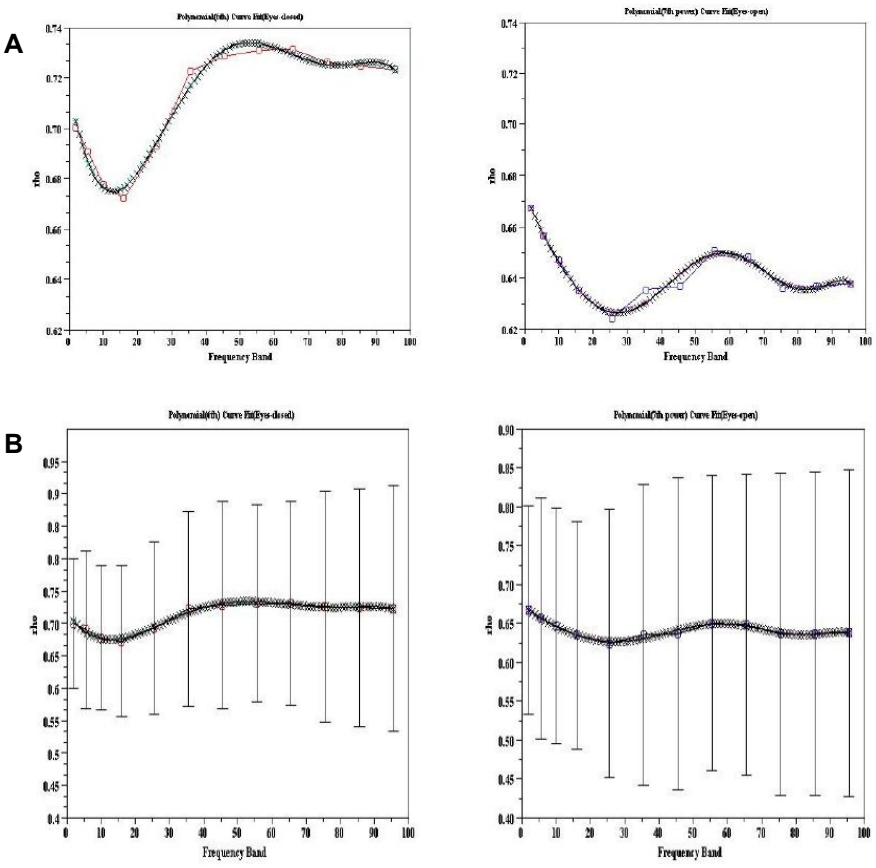

Figure 1. A. Polynomial fits for the frequency dependence of the mean Kuramoto parameter, ρ, for eyes closed (left panel)and eyes open (right panel) conditions. B. Polynomial fits (with error bars) for the frequency dependence of the mean Kuramoto parameter, ρ, for eyes closed (left panel)and eyes open (right panel) conditions.

significance (Ebersole and Pedley 2003)

- *Delta* $(\delta : f \le 4\ Hz)$. These frequencies are characteristic of deep sleep stages.
- *Theta* $(\theta : 4 < f < 8\ Hz)$. It is seen normally in young children. It may be seen in drowsiness or arousal in older children and adults. In the awake adult, high theta activity is considered abnormal and it is related to different brain disorders.
- *Alpha* $(\alpha : 8 \le f \le 12\ Hz)$. Hans Berger named the first rhythmic EEG activity he saw as the "alpha wave". They are best seen with eyes closed and are most pronounced in occipital locations.
- *Beta* $(\beta : 12 < f < 30\ Hz)$. They are best defined in central and frontal locations. They have less amplitude than alpha waves and they are enhanced upon expectancy states or tension.
- *Gamma* $(\gamma : f \ge 30\ Hz)$. Gamma rhythms represent binding of different populations of neurons together into a network for the purpose of carrying out a certain cognitive or motor function.

Filtering

The contributions of the frequency bands described above as well as those of more evenly spaced bands which are more useful in studying the frequency dependence of the EEG are extracted from the recorded signals by digital, Fourier transform (FFT)-based band-pass filters (see, e.g., Press et al. 2002). The filter function we used was an unnormalized Gaussian centered at the mid-point of the passband; the filter cutoffs were at frequencies corresponding to the half-maximum points of the filter function.

Hilbert Transform and Kuramoto Model

Phases can be associated with a real function, $x(t)$, by means of the Hilbert Transform, $h(t)$, defined by

$$h(t) = PV \int_{-\infty}^{+\infty} \frac{X(s)}{t-s} ds \qquad (1)$$

PV means the principal value of the integral. The functions, $x(t)$ and $h(t)$, are the real and imaginary parts of a complex function, $f(t)$:

$$f(t) = x(t) + ih(t) = Ae^{i\phi(t)} = A\left(\cos\phi(t) + i\sin\varphi(t)\right) \qquad (2)$$

Hence, to each real function of time, $x(t)$, we can associate the phases,

$$\phi(t) = arctan\left(\frac{h(t)}{x(t)}\right) \qquad (3)$$

For a multi-channel signal consisting of K channels, each channel having N elements, $x_m(k)$, $m = 1, 2, \ldots, K$; $k = 1, 2, \ldots, N$, we use discrete-time versions of the above equations to define K sets of phases, $\phi_m(k)$. Here, k is the discrete time variable.

Define $\rho(k)$ and $\psi(k)$ in terms of the phases, $\phi(k)$:

$$\rho(k)e^{\iota\psi(k)} = \frac{1}{K}\sum_{m=1}^{K} e^{\iota\phi(k)} \qquad (4)$$

$\rho(k)$ provides a measure of the instantaneous synchronization of the signals. Kuramoto's parameter, ρ, a measure of the synchronization of the K signals during the entire time N spanned by the signals, is defined as the average of the $\rho(k)$'s:

$$\rho = \frac{1}{N}\sum_{k=1}^{N} \rho(k) \qquad (5)$$

DATA ACQUISITION

The data used in this study were obtained by Watanabe in 1999 and 2000 using Instep (Watanabe et al. 2003). EEG signals were recorded from 16 channels referenced to linked earlobes. Table 1 shows the channel numbers and the corresponding location on the head as specified by the 10-20 system. Vertical and horizontal eye movements were recorded, respectively, from electrode sites above and below the right eye from near the canthi of each eye. Since the physical pattern of anatomical

connections is relatively stable at shorter time scales, each data file was taken no more than twelve seconds long. Artifact-corrupted records were removed from the analyses. Electrical impedances were all less than 5Kohm. Signals were amplified with a gain of 18000 and amplifier cut-off settings of 0.03 Hz and 200 Hz. Signals were digitized at 1024 Hz using a twelve-bit digitizer.

Thirteen healthy adults participated in the study. The EEG data were obtained under two conditions: eyes-closed resting and eyes-open resting. Continuous artifact-free records were obtained from each subject in the two conditions (eyes open and eyes closed). However, since the electrocap gave poor quality data in some channels, only ten channels were used in the study (see Table 1).

Table 1 shows 16 channels even though only ten are used in the calculations.

RESULTS AND DISCUSSIONS

Frequency dependence of phase synchronization

The clinically defined frequency bands are of such disparate sizes that they are not well-suited to study the frequency dependence of ρ. Consequently, we subdivided the frequency range of 0 to 100 Hz into twelve bands, keeping the delta, theta and alpha bands intact, but subdividing the beta and gamma bands essentially into 10-Hz intervals to get the following:

δ (0-4 Hz), θ (4-7 Hz), α (8-12 Hz),β1 (12-20 Hz), β2 (20-30 Hz), γ1 (30-40 Hz), γ2 (40-50 Hz), γ3 (50-60 Hz), γ4 (60-70 Hz), γ5 (70-80 Hz), γ6 (80-90 Hz) and γ7 (90-100 Hz). We (1) used bandpass filters to extract the contribution of each of these bands, (2) calculated the phases of each filtered signal using the Hilbert transform, and then (3) used these phases to calculate Kuramoto's ρ.

In Figure 1, the open circles on the left panel show the values of ρ averaged over all subjects for the eyes open condition; those on the right panel show average values for the eyes closed condition. The rather complex functional dependence of ρ on frequency can be fitted by a seventh-order polynomial for eyes open, and by a sixth order polynomial for eyes closed. In both of these cases, the best fit is that which minimizes the mean square difference between the data and the fitting polynomial.

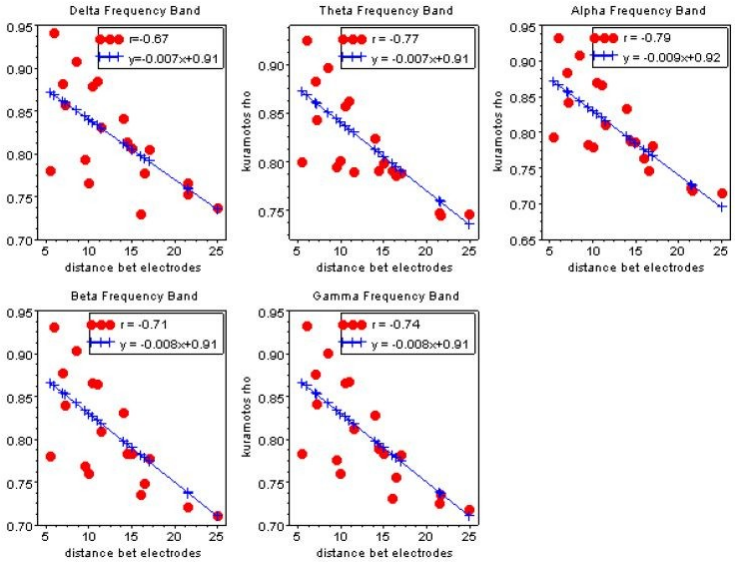

Figure 2. Scatter plot of mean Kuramoto's ρ vs. distance for all channel pairs under eyes closed condition. Top row, left to right: δ, θ, α. Bottom row, left to right: β, γ.

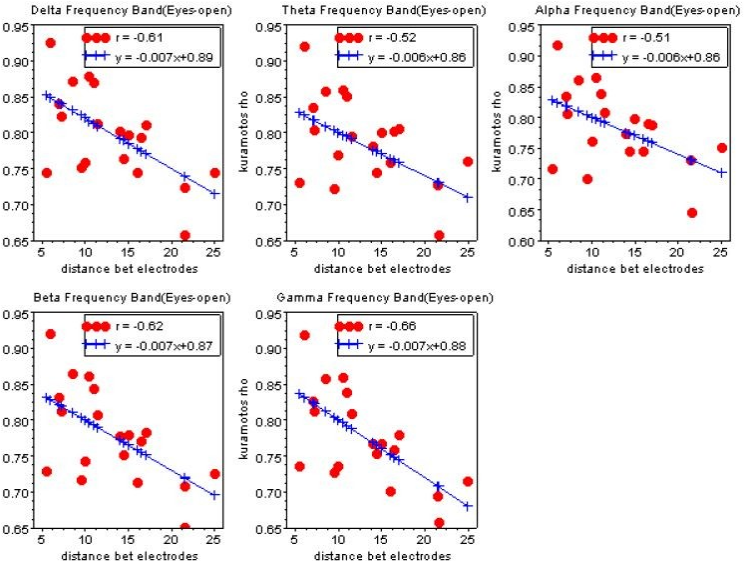

Figure 3. Same as Figure 2 but for eyes open.

For eyes open, the best fit is given by:

$$\hat{y} = -0.006x^7 - 0.007x^6 + 0.026x^5 + 0.033x^4 - 0.044x^3 - 0.039x^2 + 0.026x + 0.64 \quad (6)$$

$$\hat{y} = 0.005x^6 - 0.011x^5 - 0.004x^4 + 0.030x^3 - 0.030x^2 + 0.004x + 0.731 \quad (7)$$

where x represents the midpoint of the frequency band and $\hat{y}$ is the predicted Kuramoto's ρ. For the eyes closed condition the curve that gives the best fit has the equation

The graphs for these polynomials are shown by the smooth curves in each panel of Figure 1.

Correlation between inter-electrode distances and Kuramoto's parameter

To investigate the dependence of ρ on inter-electrode distance, we calculated the parameter at each of the five clinical frequency bands for all channel pairs and averaged these over all subjects. In the absence of inter-electrode distance data for each of the subjects, we measured the distance between each of the forty-five pairs of 10-20 electrode locations on an adult human head (Table 2). Although the source of the inter-electrode distances was not one of the subjects who provided the EEG data, we believe that the distances we used provide at least a reasonable approximation of the average inter-electrode distances among the subjects of the EEG study.

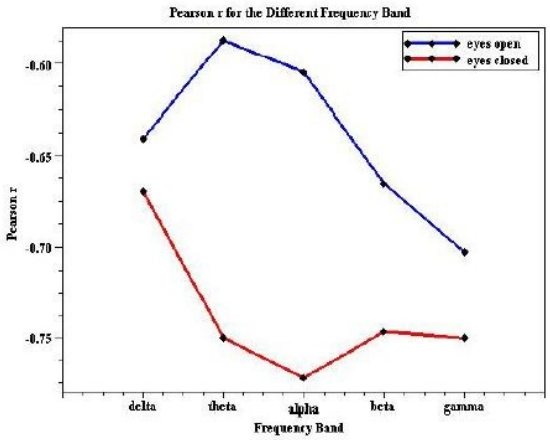

Figure 4. Cross-correlation coefficients of ρ and inter-electrode distance vs. frequency.

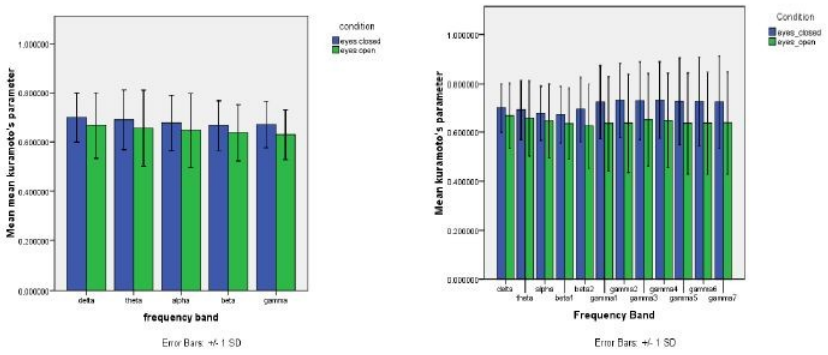

Figure 5. Mean Kuramoto's ρ vs. frequency for eyes closed and eyes open conditions. Left panel uses physiological frequency bands; right panel uses an expanded number of bands for greater resolution.

The values of Kuramoto's ρ of electrode pairs with the same distances were averaged for both conditions at each frequency band. For each of the frequency bands, the scatter plots of ρ vs. frequency for all electrode pairs are shown in Figures 2 and 3. These figures also show regression lines, the cross correlation coefficient (Pearson's r) between inter-electrode distance and the mean Kuramoto's parameter, and the regression equations.

Figures 2 and 3 show that distance between electrodes is negatively correlated with phase synchronization. The test for significance showed that the correlation coefficients are statistically significant for both conditions in the five frequency bands. Correlation analysis showed that in the eyes closed condition in the delta band, (r = -0.674, p = 0.002); theta band, (r = -0.776, p < 0.001); alpha band, (r = -

0.790, $p < .001$), beta, ($r = -0.752$, $p < 0.001$) and gamma, ($r = -0.753$, $p < .001$). On the other hand, in the eyes open condition at the delta band, ($r = -0.611$, $p = 0.005$); theta band, ($r = -0.520$, $p = 0.002$); alpha, ($r = -0.514$, $p = 0.024$); beta, ($r = -0.620$, $p = 0.005$); and gamma band, ($r = -0.663$, $p = 0.002$)

Figure 4 shows the cross-correlation coefficients of ρ and inter-electrode distance vs. frequency. This graph reveals that the anticorrelation between inter-electrode distance and Kuramoto's parameter is consistently greater in the eyes closed condition. The greatest anticorrelation occurs at the alpha band in the eyes closed condition; the lowest occurs in this band in the eyes open condition. The t-test shows that in the eyes closed condition, the signals are significantly more anticorrelated with inter-electrode distance than those in the eyes open condition ($t = -.491$, $p = .003$). Activation of the visual system apparently makes phase synchronization between brain regions less dependent on the distance between the regions.

Mean Phase Synchronization in the Different Frequency Bands

The mean phase synchronization was computed by taking the average of Kuramoto's parameter in all thirteen subjects. Figure 5 (left panel) shows an error bar chart of the average Kuramoto's parameter for the five frequency bands. Visual inspection of the figure shows that mean Kuramoto's ρ in the eyes-closed condition is higher compared to eyes-open condition for all frequency bands. It also shows that the highest mean phase synchronization occurs in the delta band in both conditions. Along this vein, while Kuramoto's ρ is sensitive to change between the eyes open versus eyes closed conditions for all frequency bands, the differences as assessed by a t-test showed that this difference is not statistically significant for the five different frequency bands. That is, at delta, ($t = 0.706$, $p = 0.487$); theta, ($t = 0.620$, $p = 0.541$); alpha, ($t = 0.590$, $p = 0.561$); beta, ($t = 0.702$, $p = 0$ .490); and gamma, ($t = 1.090$, $p = 0.286$). The graph also shows that in the different frequency bands mean phase synchronization showed different values. It can be seen that in both conditions the highest mean phase synchronization occurs at the delta band. The differences in the mean phase synchronization in the different frequency bands was assessed using one-way ANOVA .The results showed that these differences are not statistically significant for the eyes-closed condition ($F(4,60) = 0.214$, p = 0 .930) and in the eyes-open condition $F(4,60) = 0$ .165, $p = 0$ .955)

A similar analysis using the frequency bands used for evaluating frequency dependence is shown on the right hand panel of Figure 5 and yields the same results. While there are clearly visible differences between frequency bands for each condition and even larger differences between conditions, statistical analysis shows that, most likely because of large inter-subject variations, these differences are not significant.

CONCLUSIONS

This study revealed that phase synchrony of EEG signals measured at different scalp sites as quantified by Kuramoto's parameter, ρ, has a rather complicated frequency dependence, and that this dependence changes when the visual system is activated. With the eyes closed, the frequency dependence is described by a 6th order polynomial; with the eyes open, by a 7th order polynomial. In general, the phase synchronization between electrode sites is inversely proportional to the inter-electrode distance. The anticorrelation between phase synchronization and inter-electrode distance is greater when the visual system is not activated. There are noticeable differences in the average phase synchronization patterns between eyes open and eyes closed conditions, but inter-subject variations in this study were so great that the differences were not statistically significant.

The results of Figure 2 and Figure 3 obtained with these data indicate that synchronization as assessed by the Kuramoto

Table 1. Electrode locations with corresponding channel numbers. Only Channels 2 – 11 were used.

Channel	1	2	3	4	5	6	7	8	9	10	11	12	13	14	15	16
Location	H-EOG	Fz	Cz	Pz	Oz	F3	F4	C3	C4	P3	P4	T3	T4	F7	F8	V-EOG

Table 2. Inter-channel distances between all channel pairs used in this study.

Distance (cm)	Channel	Distance(cm)	Channel	Distance(cm)	Channel
5.5	Fz-F3	9.5	Fz-C3	15	C3-Oz
5.5	Fz-F4	10	Fz-C4	16	F3-C4
6	P3-Pz	10	F3-F4	16	F4-C3
6	P4-Pz	10	F3-Cz	16.5	F3-Pz
7	F3-C3	10	F4-Cz	17	Fz-P3
7	F4-C4	10.5	Cz-P4	17	Fz-P4
7	P3-Oz	10.5	C3-Pz	17	F4-Pz
7	P4-Oz	10.5	P3-P4	17	C3-C4
7.2	Fz-Cz	11	C4-Pz	17	C3-P4
7.2	Cz-C4	11.5	Cz-P3	17	C4-P3
7.2	Cz-C3	14	C4-Oz	21.5	F3-Oz
7.2	Cz-Pz	14.4	Fz-Pz	21.5	F4-Oz
7.2	Pz-Oz	14.4	Cz-Oz	21.6	Fz-Oz
8.5	C3-P3	15	F3-P3	25	F3-P4
8.5	C4-P4	15	F4-P4	25	F4-P3

order parameter decreases with distance for all frequency bands. Prior research on frequency-distance relationships in the central nervous system indicates that high frequency synchronization organizes local networks, while low frequency synchronization organizes long distance interactions (von Stein and Sarnthein 2000; Buzsáki and Draguhn 2004; Penttonen and Buzsáki 2003). These observations are consistent with theoretical calculations performed by Kopell et al. (2000). That analysis found that different frequency oscillations use different dynamical mechanisms to synchronize. Beta frequency oscillations, they concluded, synchronize over longer distances, and gamma frequency oscillations synchronize over shorter distances. These previous theoretical and experimental results would therefore seem to be at variance with the results presented here, which show synchronization decreasing with distance over all frequency bands. We think it possible that this difference results from examining free running EEGs, as is done here, in contrast with examining event-related potentials, ERPs, as was done for example by von Stein and Sarnthein (2000). Event-related potentials are electrical signals that are elicited by defined brief stimuli. The stimulus engages the CNS is a reproducible perceptual and cognitive task, and focuses CNS activity in a way that permits stimulus-specific resolution of frequency-distance relationships.

This argues for the application of the Kuramoto order parameter to the analysis of event-related potentials. The first step of the analysis would be the identification of transient functional networks formed in response to the stimulus. Several methods can be used to identify functional networks in multichannel EEG/ERP data. Linear and nonlinear time domain measures can be used (Bonita et al. 2012), but since the object of the study is to examine frequency relationships, frequency domain measures of functional connectivity would be more appropriate. Frequency domain measures of functional connectivity include coherence (Nunez et al. 1997, 1999; though previously reported problems with the calculation of coherence (Schiff 2005; Guevara et al. 2005) should be noted), phase locking index (Hurtado et al. 2004; Sazonov et al. 2009), imaginary coherency (Stam et al. 2007; Nolte et al. 2004), and phase lag index (Stam et al. 2007, 2009). The search for transient functional networks should be repeated in each frequency band. Stimulus-dependent Kuramoto order parameters can then be computed within the networks identified by the preceding functional connectivity analysis.

ACKNOWLEDGMENTS

MCF acknowledges support from Xavier University and the Commission on Higher education, Republic of the Philippines. AMA is grateful for the support of the Balik Scientist Program of the Department of Science and Technology, Republic of the Philippines he also thanks Mindanao State University – Iligan Institute of Technology for their hospitality.

This research was supported in part by the Traumatic Injury Research Program of the Uniformed Services University (Bethesda, MD, USA.), the Marine Corps Systems Command, and the Defense Medical Research and Development Program. The opinions and assertions contained herein are the private ones of the authors and are not to be construed as official or reflecting the views of the U. S. Department of Defense.

REFERENCES

Acebrón JA, Bonilla LL, Perez Vicente CJ, Ritort F, SpiglerR. A simple paradigm for synchronization phenomena: The Kuramoto model. Rev Mod Phys 2005; 77:137-185.

Albano AM, Brodfuehrer PD, Cellucci CJ, Tigno XT, Rapp PE. Time series analysis, or the quest for quantitative measures of time dependent behavior. Phil Sci Letts 2008; 1:18-31.

Albano AM, Cellucci CJ, Harner RJ, Rapp PE. Optimization of embedding parameters for prediction of seizure onset with mutual information. In Mees AI, ed. Nonlinear Dynamics and Statistics, Boston: Birkhaeuser, 2000: 435-451.

Bonita JD, Ambolode LCC, Rosenberg BM, Cellucci CJ, Watanabe TAA, Rapp PE, Albano AM. Time domain measures of CNS functional connectivity: a comparison of linear, nonparametric and nonlinear measures. 2012 (manuscript in preparation).

Brazier MAB, Casby JU. Crosscorrelation and autocorrelation studies of electroencepha-lographic potentials. Electroenceph Clin Neurophys 1952; 4:201-211.

Buzsáki G, Draguhn A. Neuronal oscillations in cortical networks..Science.2004; 304:1926-1929.

Ebersole JS, Pedley TA. Current Practice of Clinical Electroencephalography. Third Edition. Philadelphia, PA: Lippincott, Williams and Wilkins, 2003.

Fraser AM, Swinney HL. Independent coordinates for strange attractors from mutual information. Phys Rev A 1986; 33:1134-1140.

Gevins AS, Remond A. eds. Methods of Analysis of Brain Electrical and Magnetic Signals: EEG Handbook. Amsterdam: Elsevier Science, 1987.

Granger CWJ. Investigating causal relations by econometric models and cross-spectral methods. Econometrica 1969; 37:424-438.

Guevara R, Pérez Velazquez JL, Nenadovic V, Wennberg R, Senjanović G, Dominguez LG. Phase synchronization measurements using electroencephalographic recordings. What can we really say about neuronal synchrony? Neuroinformatics 2005; 3:301-313.

Hahn SL. Hilbert Transforms in Signal Processing. New York: Wiley, 1996.

Hurtado JM, Rubchinskiy LL, Sigvardt KA. Statistical method for detecting of phase locking episodes in neural oscillations. J Neurophys 2004; 91:1883-1898.

King FW. Hilbert Transforms. Cambridge: Cambridge University Press, 2009.

Kopell N, Ermentrout GB, Whittington MA, Traub RD. Gamma rhythms and beta rhythms have different synchronization properties. Proc Natl Acad Sci USA 2000; 97:1867-1872.

Kuramoto Y. Self-entrainment of a population of coupled nonlinear oscillators. In: H. Araki, ed. International

Symposium of Mathematical Problems in Theoretical Physics, 39. Berlin: Springer Verlag, 1975: 420-422.

Kuramoto Y. Chemical Oscillations, Waves and Turbulence. Berlin: Springer Verlag, 1984.

Madulara MD, Francisco PAB, Nawang, S, Arogancia DC, Cellucci CJ, Rapp PE, Albano AM. EEG transfer entropy tracks changes of information transfer on the onset of vision. International Journal of Modern Physics 2012 (in press).

Mars NJI, Lopes da Silva FH. In: Gevins AS, Remond A. eds. Methods of Analysis of Brain Electrical and Magnetic Signals: EEG Handbook. Amsterdam: Elsevier Science, 1987.

Nolte G, Bai O, Wheaton L, Mari Z, Vorbach S, Hallet M. Identifying true brain interaction from EEG data using the imaginary part of coherency. Clin Neurophysiol 2004; 115:2292-2307

Nunez PL, Silberstein RB, Shi ZP, Carpenter MR, Srinivasan R, Tucker DM, Doran SM, Cadusch PJ and Wijesinghe RS. EEG coherency: II. Experimental comparisons of multiple measures.Clinical Neurophsyiology 1999; 110: 469-486.

Nunez PL, Srinivasan R, Westdorp AF, Wijesinghe RS, Tucker DM, Silberstein RB, Cadusch PJ. EEG coherency. I. Statistics, reference electrode, volume conduction, Laplacians, cortical imaging and interpretation at multiple scales. Electroencephalogr Clin Neurophsyiol 1997; 103:499-515.

Penttonen M, Buzsáki G. Natural logarithmic relationship between brain oscillators. Thalamus and Related Systems 2003; 2:145-152.

Press WH, Teukolsky SA, Vetterling WT, Flannery BP. Numerical Recipes in C++. New York: Cambridge University Press, 2002.

Sazonov AV, Ho CK, Bergmans JWM, Arends JBAM, Griep PAM, Verbitskiy EA, Cluitmans PJM, Boon PAJM. An investigation of phase locking index for measuring interdependency of cortical source signals recorded in the EEG. Biol Cyben 2009; 100:129-146

Schiff SJ. Dangerous phase. Neuroinformatics 2005; 3:315-318.

Sakaguchi H, Kuramoto Y. A Soluble Active Rotater Model Showing Phase Transitions via Mutual Entertainment. Progr Theoret Phys 1986; 75:1105-1110

Schreiber T. Measuring Information Transfer. Phys Rev Lett 2000; 85:464-464.

Stam CJ, Nolte G, Daffertshofer A. Phase lag index: Assessment of functional connectivity from multichannel EEG and MEG with diminished bias from common sources. Hum Brain Mapp 2007; 28:1178-1193.

Stam CJ, de Haan W, Daffertshofer A, Jones BF, Manshanden I, van Cappellen van Walsum AM, Montez T, Verbunt JPA, de Munck JC, van Dijk BW, Berendse HW, Scheltens P. Graph theoretical analysis of magentoencephalographic functional connectivity in Alzheimer's disease. Brain 2009; 132:213-224.

von Stein A, SarntheinJ. Different frequencies for different scales of cortical integration: from local gamma to long range alpha/theta synchronization. Int J Psychophysiol 2000; 38:301-313.

Strogatz SH. From Kuramoto to Crawford: Exploring the onset of synchronization in populations of coupled oscillators. Physica D 2000; 143:1–20.

Watanabe TAA, Cellucci CJ, Kohegyi E, Bashore TR, Josiassen RC, Greenbaun NN, Rapp PE. The algorithmic complexity of multichannel EEGs is sensitive to changes in behavior. Psychophysiology 2003; 40:77-97.

Xu J, Liu ZR, Yang QF. Information transmission in human cerebral cortex. Physica D 1997; 106:363-368.